Available online at www.sciencedirect.com
SCIENCE DIRECT®
Journal of Sound and Vibration 283 (2005) 685–706
JOURNAL OF SOUND AND VIBRATION
www.elsevier.com/locate/jsvi

Active aeroelastic control of 2-D wing-flap systems operating in an incompressible flowfield and impacted by a blast pulse

Liviu Librescu[a,*], Sungsoo Na[b], Piergiovanni Marzocca[c], Chanhoon Chung[b], Moon K. Kwak[d]

[a]*Department of Engineering Science and Mechanics, Virginia Polytechnic Institute and State University, Blacksburg, VA 24061-0219, USA*
[b]*Korea University, 136-701 Seoul, Republic of Korea*
[c]*Clarkson University, Potsdam, NY 13699-5725, USA*
[d]*Dongkuk University, Jung-gu, Seoul, Republic of Korea*

Received 1 April 2003; accepted 7 May 2004

Abstract

This paper concerns the active aeroelastic control of 2-D wing-flap systems operating in an incompressible flowfield and exposed to a blast pulse. The goal is to implement an active flap control capability to suppress the flutter instability and enhance the subcritical aeroelastic response to time-dependent external pulses. To this end, a combined control law is implemented and its performances toward suppressing flutter and reducing the vibrational level in the subcritical flight speed range is demonstrated.

1. Introduction

The next generation of combat aircraft is likely to operate in more severe environmental conditions than in the past. This implies that such an aircraft will be exposed to blasts, fuel explosions, sonic-booms, etc. [1,2].

*Corresponding author. Tel.: +1-540-231-5916; fax: +1-540-231-4574.
E-mail address: librescu@vt.edu (L. Librescu).

0022-460X/$ - see front matter © 2004 Elsevier Ltd. All rights reserved.
doi:10.1016/j.jsv.2004.05.010

Nomenclature

$\mathbf{A}$	system matrix for first-order differential equation
A_i, B_i	aerodynamic lag state variables
$\mathbf{A}_{ij}$	submatrix of A
α	elastic pitch angle
α_1, α_2	coefficients of the two-term approximation of the Wagner function
b	semi-chord
$\mathbf{B}$	control input matrix
β	flap angle
β_1, β_2	coefficients of the two-term approximation of the Wagner function
c	dimensionless distance to flap hinge line from the elastic axis
$\mathbf{C}$	state matrix
$C(k)$	Theodorsen's function
d	dimensionless distance to elastic axis from leading edge
$D(t)$	Duhamel's integral
$\Phi(tV_f/b)$	Wagner's function
$\mathbf{G}$	disturbance-input matrix
$g_{\dot{h}}, g_{\dot{\alpha}}$	velocity control gains in plunge and pitch
h	plunging displacement
i	$\sqrt{-1}$
I_α, I_β	inertia in pitch and of the aileron
$\mathbf{K}$	stiffness matrix
$\mathbf{K}_C$	gain matrix
K_α, K_β, K_h	stiffness of pitch, flap and plunge spring
L, M	lift and aerodynamic moment
$\mathbf{M}$	mass matrix
m	mass of airfoil
$P(t)$	Duhamel's integral
ρ	air density
S	static moment
S_α, S_β	static moment of pitch and flap angles
σ	dummy time variable
T	unsteady torque moment of flap spring
t	time
$\mathbf{u}$	control vector
V_f, V_F	flight and flutter speeds, respectively
x, y	horizontal and vertical coordinates
x_{EA}	elastic axis position from the mid-chord, positive rearward
$\mathbf{Y}$	column vector of plunge, pitch, and flap displacements
w_G	vertical gust velocity
w	external disturbance
$(\cdot)'; (\cdot)''$	$= \mathrm{d}(\cdot)/\mathrm{d}\tau; = \mathrm{d}^2(\cdot)/\mathrm{d}\tau^2$
$\dot{(\cdot)}, \ddot{(\cdot)}$	$= \mathrm{d}(\cdot)/\mathrm{d}t; = \mathrm{d}^2(\cdot)/\mathrm{d}t^2$
$[\cdot]^{\mathrm{T}}$	transpose of a matrix

Under such circumstances, even in the conditions of subcritical flight, the wing structure will be subjected to large oscillations that can result in its failure by fatigue. Moreover, in some special events occurring during its operational life, such as escape maneuvers, significant decays of the flutter speed can occur with dramatic implications for its structural integrity. Passive methods which have been used to address this problem include added structural stiffness, mass balancing, and speed restrictions. However, all these attempts to enlarge the operational flight envelope and to enhance the aeroelastic response result in significant weight penalties, or in unavoidable reduction of nominal performances. All these facts fully underline the necessity of the implementation of an active control capability enabling one to fulfill two basic objectives: (1) to enhance the subcritical aeroelastic response, in the sense of suppressing or even alleviating the severity of the wing oscillations in the shortest possible time, and (2) to expand the flight envelope by suppressing flutter instability and so, of contributing to a significant increase of the allowable flight speed. With this in mind, in this paper the active aeroelastic control of a 2-D wing-flap system operating in an incompressible flowfield and impacted by a blast will be investigated. This

model is able to capture most of the dynamics of a 3-D wing and for this reason is still well used in linear and nonlinear analyses [3,4]. On the other hand, a clear understanding of control mechanism is of vital importance for complex wing configurations. Moreover, this study can be viewed as a preliminary work in the context of the morphing wing technology.

In the last two decades, the advances of the active control technology have rendered the applications of active flutter suppression and active vibrations control systems feasible [3–8]. A great deal of research activity devoted to the aeroelastic active control and flutter suppression of flight vehicles has been accomplished. Excellent state-of-the-art discussions of these issues are presented in Refs. [6,7]. The reader is also referred to a sequence of articles appeared in the Journal of Guidance, Control and Dynamics [8] where a number of recent contributions related to the active control of aircraft wing are discussed in detail.

In a classical sense, the active flutter and vibration suppression control is based on the use of a control surface as a primary control. Its deflection is commanded by a suitable control law, i.e. by a relationship between the motion of the 2-D wing section and the control surface deflection. In the present paper, several control strategies, i.e. plunging/pitching velocity feedback control and their combination, linear-quadratic regulator (LQR) [9–11], modified bang–bang (MBB) [12] and fuzzy logic control (FLC) [13] are implemented, and some of their relative performances are put into evidence. From a physical point of view, the active control is achieved by deflecting the control surface in a manner that alters the overall nature of the aerodynamic forces on the wing, as to change in a beneficial way the aeroelastic behavior of the wing structure.

In the present paper, corresponding to time-dependent arbitrary motions of a 3-dof airfoil featuring plunging–pitching–aileron deflection, the aerodynamic forces are derived from Theodorsen's equations using Wagner's function. The equations of motion are presented in state-space form, suitable for control purposes.

2. Configuration of the 2-D wing-flap structural model

Fig. 1 shows the typical wing-flap section that is considered in the present analysis. This model has been well established for 2-D aeroelastic analyses, see e.g. Refs. [14,15]. The 3-dof associated with the airfoil appear clearly from Fig. 1. The pitching and plunging displacements are restrained by a pair of springs attached to the elastic axis of the airfoil (EA) with spring constants K_α and K_h, respectively.

The aerodynamically unbalanced control flap is located at the trailing edge. A torsional flap spring is also attached at the hinge axis of the control surface whose spring constant is K_β; h denotes the plunge displacement (positive downward), α the pitch angle (measured from the horizontal at the elastic axis of the airfoil, positive nose-up) and β is the aileron deflection (measured from the axis created by the airfoil at the control flap hinge, positive flap-down).

3. Governing equations of the aeroelastic model

The governing equations pertinent to the 3-dof aeroelastic systems are available in the classical aeroelasticity monographs. In matrix form the equations governing the aeroelastic motion of a

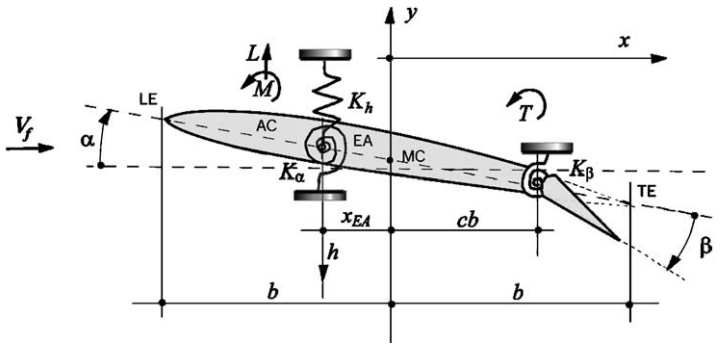

Fig. 1. Typical wing-flap section.

2-D wing–aileron system can be written as [15,16]

$$\mathbf{M}\ddot{\mathbf{Y}}(t) + \mathbf{K}\mathbf{Y}(t) = -\mathbf{L}(t) - \mathbf{L}_g(t) + \mathbf{L}_b(t) + \mathbf{L}_c(t), \tag{1}$$

where $\mathbf{L}(t)$, $\mathbf{L}_g(t)$, $\mathbf{L}_b(t)$ and $\mathbf{L}_c(t)$ represent the unsteady aerodynamic, gust, blast and control loads, respectively. In this equation the column vector of plunging/pitching/flapping displacements is defined as

$$\mathbf{Y}(t) = \left\{ \frac{h(t)}{b} \quad \alpha(t) \quad \beta(t) \right\}^{\mathrm{T}}, \tag{2}$$

while

$$\mathbf{M} = \begin{bmatrix} bm & S_\alpha & S_\beta \\ bS_\alpha & I_\alpha & I_\beta + bcS_\beta \\ bS_\beta & I_\beta + bcS_\beta & I_\beta \end{bmatrix}, \quad \mathbf{K} = \begin{bmatrix} bK_h & 0 & 0 \\ 0 & K_\alpha & 0 \\ 0 & 0 & K_\beta \end{bmatrix} \tag{3}$$

denote the mass, and stiffness matrices, respectively.

The second-order aeroelastic governing equation can be cast in a first-order state-space form as

$$\dot{\mathbf{X}}(t) = \mathbf{A}\mathbf{X}(t) + \mathbf{B}\mathbf{u}(t) + \mathbf{G}_g\mathbf{w}_g(t) + \mathbf{G}_b\mathbf{w}_b(t). \tag{4}$$

Here $\mathbf{A}$ is the aerodynamic matrix; see Appendix A. The state vector is given by

$$\mathbf{X}(t) = \left\{ \dot{h}(t)/b \quad \dot{\alpha}(t) \quad \dot{\beta}(t) \quad h(t)/b \quad \alpha(t) \quad \beta(t) \quad B_1(t) \quad B_2(t) \quad A_1(t) \quad A_2(t) \right\}^{\mathrm{T}}. \tag{5}$$

$B_1(t), B_2(t), A_1(t)$ and $A_2(t)$ are the aerodynamic-lag states; $\mathbf{u}(t)$ is the control input, while $\mathbf{w}_g(t), \mathbf{w}_b(t)$ are external disturbances represented in the present case by a time-dependent external excitation, such as a gust load (identified by a subscript g), an explosive blast, sonic-boom or step pressure pulses (identified by a subscript b):

$$\mathbf{w}_g(t) = \{w_L(t) \quad w_M(t) \quad w_T(t)\}^{\mathrm{T}}, \quad \mathbf{w}_b(t) = \{f(t) \quad 0 \quad 0\}^{\mathrm{T}}, \tag{6}$$

where $f(t) = P_m(1 - t/t_p)[H(t) - H(t - rt_p)]$; see Ref. [1]; $\mathbf{G}_g, \mathbf{G}_b$ are the disturbance-input matrix ($\mathbf{G}_g = \mathbf{G}_b$; see Appendix A), while $\mathbf{B}$ is the control input matrix that is given by

$$\mathbf{B} = \frac{1}{I_\beta}\{\{\mathbf{M}^{-1}\{0 \quad 0 \quad 1\}^{\mathrm{T}}\}^{\mathrm{T}} \quad 0 \quad 0 \quad 0 \quad 0 \quad 0 \quad 0 \quad 0\}^{\mathrm{T}}. \tag{7}$$

In the present approach, different types of control methodologies have been applied, such as plunging/pitching and combination of velocity feedback controls, LQR, MBB and FLC.

For stability purpose, an infinite-time LQR that leads to a full state-feedback controller of the form $\mathbf{u}(t) = -\mathbf{K}_C\mathbf{X}$, has been used. Herein, $\mathbf{K}_C$ is the feedback gain matrix, while $\mathbf{X}$ is the full state vector to be defined next. In particular, we use the Riccati equation to solve for an optimal control $\mathbf{u}_{\mathrm{opt}}$.

The aerodynamic load vector appearing in Eq. (1) is expressed in terms of its components as

$$\mathbf{L}(t) = \{\, L(t) \quad M(t) \quad T(t)\,\}^{\mathrm{T}}, \tag{8}$$

where L, M and T denote, respectively, the aerodynamic lift (positive in the upward direction), the pitching moment about the one-quarter chord of the airfoil (positive nose-down), and the flap torque applied to the flap hinge.

For the gust loading, following Ref. [17],

$$\mathbf{L}_g(t) = \{\, L_G(t) \quad M_{yG}(t) \quad T_T(t)\,\}^{\mathrm{T}} = \int_0^t \{\, I_{LG}(t-\sigma) \quad I_{MG}(t-\sigma) \quad I_{fG}(t-\sigma)\,\}^{\mathrm{T}} \frac{w_G}{V_f}\,\mathrm{d}\sigma, \tag{9}$$

where w_G is the gust vertical velocity, while I_{LG}, I_{MG} and I_{fG} are the related aerodynamic indicial functions. For the incompressible flow, these are expressed as

$$\{\, I_{LG}(t-\sigma) \quad I_{MG}(t-\sigma) \quad I_{fG}(t-\sigma)\,\}^{\mathrm{T}} = \{\, 4\pi\dot{\psi} \quad I_{LG}(1/2 + x_{\mathrm{EA}}/b) \quad 0\,\}^{\mathrm{T}}. \tag{10}$$

Küssner's function ψ is approximated by [17]

$$\psi(t) = 1 - 0.5\mathrm{e}^{-0.13t} - 0.5\mathrm{e}^{-t}. \tag{11}$$

In the time domain, the aerodynamic loads have the form

$$L(t) = \pi\rho b^2\left[\ddot{h}(t) - bx_{\mathrm{EA}}\ddot{\alpha}(t) + \frac{b}{2\pi}\,\Phi_4\ddot{\beta}(t) + V_f\dot{\alpha}(t) + \frac{V_f}{\pi}\,\Phi_3\dot{\beta}(t)\right] + 2\pi\rho V_f bD(t), \tag{12}$$

$$M(t) = \pi\rho b^3\left[-x_{\mathrm{EA}}\ddot{h}(t) + b\left(\tfrac{1}{8} + x_{\mathrm{EA}}^2\right)\ddot{\alpha}(t) + \frac{b}{4\pi}\,\Phi_7\ddot{\beta}(t) + \left(\tfrac{1}{2} - x_{\mathrm{EA}}\right)V_f\dot{\alpha} + \frac{V_f}{2\pi}\,\Phi_6\dot{\beta}(t) + \frac{V_f^2}{\pi b}\,\Phi_5\beta(t)\right] - 2\pi\rho b^2\left(\tfrac{1}{2} + x_{\mathrm{EA}}\right)V_f D(t), \tag{13}$$

$$T(t) = \pi\rho b^2\left[\left(\frac{b}{2\pi}\,\Phi_4\right)\ddot{h}(t) + \left(\frac{b^2}{4\pi}\,\Phi_7\right)\ddot{\alpha}(t) + \left(\frac{b^2}{2\pi^2}\,\Phi_{12}\right)\ddot{\beta}(t) + \left(\frac{bV_f}{2\pi}\,\Phi_9\right)\dot{\alpha} + \left(\frac{bV_f}{2\pi^2}\,\Phi_{11}\right)\dot{\beta}(t) + \left(\frac{V_f^2}{\pi^2}\,\Phi_{10}\right)\beta(t)\right] + \pi\rho V_f bP(t), \tag{14}$$

where $\Phi_i(\phi)$ are Theodorsen's constants [15,16], while $\phi = \arccos(-x_{\text{flap}}/b)$. These transient aerodynamic loads are obtained from a Fourier transform of the two-dimensional incompressible oscillatory coefficients, see e.g. Refs. [18,19]. The functions $D(t)$ and $P(t)$ are Duhamel integrals given by

$$\{D(t) \quad P(t)\} = \int_0^t \Phi\left[\frac{(t-\sigma)V_f}{b}\right]\{Q_1'(\sigma) \quad Q_2'(\sigma)\}\,\mathrm{d}\sigma, \tag{15}$$

where $\Phi[V_f(t-\sigma)/b]$ is Wagner's function. In addition, for a system that is initially at rest, $Q_1'(\tau)$ and $Q_2'(\tau)$ are expressed as [17,20]

$$Q_1'(\tau)\left(\equiv\frac{\mathrm{d}Q_1(\tau)}{\mathrm{d}\tau}\right) = h''(\tau) + \left(\tfrac{1}{2} - x_{\text{EA}}\right)b\alpha''(\tau) + \frac{b}{2\pi}\Phi_2\beta''(\tau) + V_f\alpha'(\tau) + \frac{V_f}{\pi}\Phi_1\beta'(\tau), \tag{16}$$

$$\begin{aligned} Q_2'(\tau)\left(\equiv\frac{\mathrm{d}Q_2(\tau)}{\mathrm{d}\tau}\right) &= \frac{b}{\pi}\Phi_8 h''(\tau) + \frac{b^2}{\pi}\left(\tfrac{1}{2} - x_{\text{EA}}\right)\Phi_8\alpha''(\tau) + \frac{b^2}{2\pi^2}\Phi_2\Phi_8\beta''(\tau) + \frac{V_f b}{\pi}\Phi_8\alpha'(\tau) \\ &\quad + \frac{V_f b}{\pi^2}\Phi_1\Phi_8\beta'(\tau) = \frac{b}{\pi}\Phi_8 Q_1'(\tau), \end{aligned} \tag{17}$$

where the dimensionless time τ is expressed as $\tau = tV_f/b$ and $(\cdot)'; (\cdot)'' = \mathrm{d}(\cdot)/\mathrm{d}\tau; = \mathrm{d}^2(\cdot)/\mathrm{d}\tau^2$. $Q_1(\tau)$ and $Q_2(\tau)$ are measures of the circulation about the airfoil with flap. The standard two-term Jones' exponential approximation of Wagner's function (incompressible flow field) is adopted here and is given by [15]

$$\Phi(\tau) = 1 - \alpha_1 \mathrm{e}^{-\beta_1\tau} - \alpha_2\mathrm{e}^{-\beta_2\tau}, \quad \alpha_1 = 0.165, \quad \alpha_2 = 0.335, \quad \beta_1 = 0.041, \quad \beta_2 = 0.32. \tag{18}$$

$D(t)$ and $P(t)$ are evaluated following the procedure highlighted in Refs. [19,20]. Substitution of Eq. (18) in Eq. (15) yields

$$\{D(t) \quad P(t)\} = \{Q_1(t) - \alpha_1 B_1(t) - \alpha_2 B_2(t) \quad Q_2(t) - \alpha_1 A_1(t) - \alpha_2 A_2(t)\}, \tag{19}$$

where $Q_1(t)$ and $Q_2(t)$ are obtained in the time domain from Eqs. (16) and (17) via integration

$$Q_1(t) = \dot{h}(t) + \dot{\alpha}(t)\left(\tfrac{1}{2} - x_{\text{EA}}\right)b + \frac{b}{2\pi}\Phi_2\dot{\beta}(t) + V_f\alpha(t) + \frac{V_f}{\pi}\Phi_1\beta(t), \tag{20}$$

$$\begin{aligned} Q_2(t) &= \frac{b}{\pi}\Phi_8\dot{h}(t) + \frac{b^2}{\pi}\left(\tfrac{1}{2} - x_{\text{EA}}\right)\Phi_8\dot{\alpha}(t) + \frac{b^2}{2\pi^2}\Phi_2\Phi_8\dot{\beta}(t) + \frac{V_f b}{\pi}\Phi_8\alpha(t) + \frac{V_f b}{\pi^2}\Phi_1\Phi_8\beta(t) \\ &= \frac{b}{\pi}\Phi_8 Q_1(t). \end{aligned} \tag{21}$$

Herein the overdots denote time derivatives with respect to t. One should remark that the aerodynamics incorporated in the model is in the form of the aerodynamic indicial function. The motivation for its use stems from the fact that it enables to obtain linearized unsteady aerodynamic loads in the time domain via Duhamel's convolution. The indicial functions can be derived via various approaches, such as rational approximation, computational fluid dynamics (CFD), or in an experimental way. Based on the concept of indicial functions, a unified representation of linear unsteady aerodynamic loads in incompressible, compressible subsonic and supersonic flows can be developed; see Refs. [21–24]. For problems related to the determination of lift and moment responses to penetration of sharp-edged traveling gusts, the reader is referred to Refs. [25–28].

4. Numerical simulation

The geometrical and physical characteristics of the 2-D wing-flap system to be used in the present numerical simulations are presented in Table 1. The flutter speed for this model is $V_F = 457\,\text{ft/s}$. In order to validate the result present in this paper a comparison is done using the parameters presented in Refs. [15,17], for which the calculated flutter speed is $V_F = 890\,\text{ft/s}$. The critical value of the flutter speed is obtained herein via the solution of both the complex eigenvalue problem and from the subcritical aeroelastic response analysis and an excellent agreement with Refs. [15,17] is reached.

Within the present simulations, due to the fact that the proportional and acceleration controls were proven to be less efficient, only combined velocity feedback control laws were used. As a result, herein, plunging/pitching velocity feedback control and their combination are used. These relate the control input $u(t)$, i.e. the required flap deflection angle, to the decoupled plunging and pitching velocities of the main airfoil surface. Hence $u(t)$ is represented according to the law

$$u(t) = g_{\dot{h}}(\dot{h}/b) + g_{\dot{\alpha}}\dot{\alpha}, \tag{22}$$

where $g_{\dot{h}}$ and $g_{\dot{\alpha}}$ are the corresponding control gains.

A more encompassing control law, that includes plunging/pitching deflections and plunging/pitching accelerations is presented in Ref. [29]. As remarked in Ref. [29], from the mathematical point of view, it can be assumed that, instead of moving the flap with a required deflection, an equivalent control hinge moment can be incorporated into the open-loop aeroelastic governing equation (4). This is analytically valid since this external moment acts on the flap-hinge and affects only the β dof.

There is no doubt that more encompassing control laws can be implemented. In this context, two optimal feedback control methodologies, namely LQR and MBB, and a FLC have been applied.

In the presence of external time-dependent excitations, the determination of the time-history of the quantities $(\widetilde{h}(\equiv h/b), \alpha, \beta)$, at any flight speed lower than the flutter speed, requires the solution of a boundary-value problem [9]. In the absence of the control input, the open-loop aeroelastic response is obtained, whereas in the presence of the control, the closed-loop aeroelastic response is derived.

Several results displaying the closed/open-loop aeroelastic response to selected types of loads are supplied next. Details on the blast, sonic-boom and gust loads are available in Refs. [1,2,9,13,23].

In Figs. 2(a) and (b), the open/closed response time-histories of the quantities $(\widetilde{h}, \alpha)$ of the aeroelastic system operating in close proximity to the flutter boundary ($V_f = 456.5\,\text{ft/s}$) and subjected to a blast load (represented in the inset of the respective figures) and characterized throughout numerical simulation by $P_m = 1.0$ lb/ft, are presented.

The result reveal that in the absence of the control, the amplitudes of the response quantities are on the verge of increasing in time, implying that the system is in close proximity to the flutter instability. However, in the presence of the plunging velocity feedback control (identified by the gain $g_{\dot{h}}$), and especially, of the combined velocity feedback control (identified by the gains $g_{\dot{\alpha}}, g_{\dot{h}}$), as time unfolds, the amplitudes decay rapidly. In this analysis, a combined plunging–pitching velocity feedback control law will produce a combination of effects, implying that this type of

Table 1
2-D wing-flap section parameters

$b = 1\,\text{ft}$	$K_h = 500\,\text{m}$
$x_{EA} = -0.3$	$K_\alpha = 2000 I_\alpha$
$c = 1.0$	$K_\beta = 18,000 I_\beta$
$m = 1.88181\,\text{slugs/ft}$	$\rho = 0.002378\,\text{slugs/ft}^3$
$I_\beta = 0.037804\,\text{slugs ft}^2/\text{ft}$	$S_\beta = 0.030243\,\text{slugs}$
$S_\alpha = 0.483894\,\text{slugs}$	$I_\alpha = 1.51217\,\text{slugs ft}^2/\text{ft}$

control law proves to be more effective than that based on either the plunging, or pitching velocity feedback control alone. In addition, it can be also shown that the pitching velocity feedback control alone is more efficient than the plunging one.

The open-loop time-histories of quantities $(\widetilde{h}, \alpha, \beta)$ of the aeroelastic system subjected to a step pulse are depicted in Fig. 3. It is clearly revealed that in this case, at the flight speed $V_f > V_F$, oscillations with exponentially growing amplitudes occur.

In Figs. 4(a)–(c) there are depicted the open-loop plunging, pitching and aileron flapping aeroelastic time-histories, exposed to a graded gust, for selected subcritical flight speeds.

In this connection, it should be noticed that, for $\widetilde{h}$ and α, higher amplitudes correspond to lower flight speeds, and, for the same quantities, the flutter appears when the oscillation amplitudes are lower than those featured at lower flight speeds. This feature was highlighted also in Refs. [1,22]. However, for β an opposite trend occurs. It is also evident that, for values of the flight speed larger than the flutter speed, oscillations with exponentially growing amplitudes occur.

This is even more evident in Fig. 5 where there are displayed the open/closed-loop plunging aeroelastic time-histories of the airfoil with flap exposed to a step pulse, for selected flight speeds. Whereas for flight speeds below the flutter speed, a very little influence of the control is visible, in the sense of a marginal influence on the time-history, at $V_f > V_F$ the flutter response is converted, by its action, into a stable response.

In Figs. 6(a)–(c) the open-loop dimensionless plunging, pitching and flapping time-histories of the aeroelastic system operating at three different flight speeds ($V_f = 400, 440\,\text{ft/s}, V_f = V_F$) and exposed to a blast pulse are presented. With the increase of the flight speed, a growth of the aeroelastic response deflection is experienced.

The counterparts of Figs. 6(a) and (b) for the open-loop system exposed to a symmetric sonic-boom ($r = 2$) for the same flight speed regime are depicted in Figs. 7(a) and (b). Similar conclusions can be reached. For a speed $V_f < V_F$, it becomes apparent that the amplitude of the response decreases with the increase of the speed. However, for $V_f = V_F$ the response becomes unbounded, implying that the occurrence of the flutter instability is impending. It should be noticed that the response to sonic-boom pressure pulses involves two regimes: one that corresponds to the forced motion, and the other that corresponds to free motion. The jump appearing in the graph is due to the discontinuity in the sonic-boom pulse occurring at $t_p = 10\,\text{s}$. For explosive pressure pulses, where $r = 1$, the jump does not occur (Figs. 6(a) and (b)).

The influence of combined velocity feedback controls on the aeroelastic response of a typical section wing with the flap exposed to an asymmetric sonic boom ($r = 1.5$) is presented in Fig. 8.

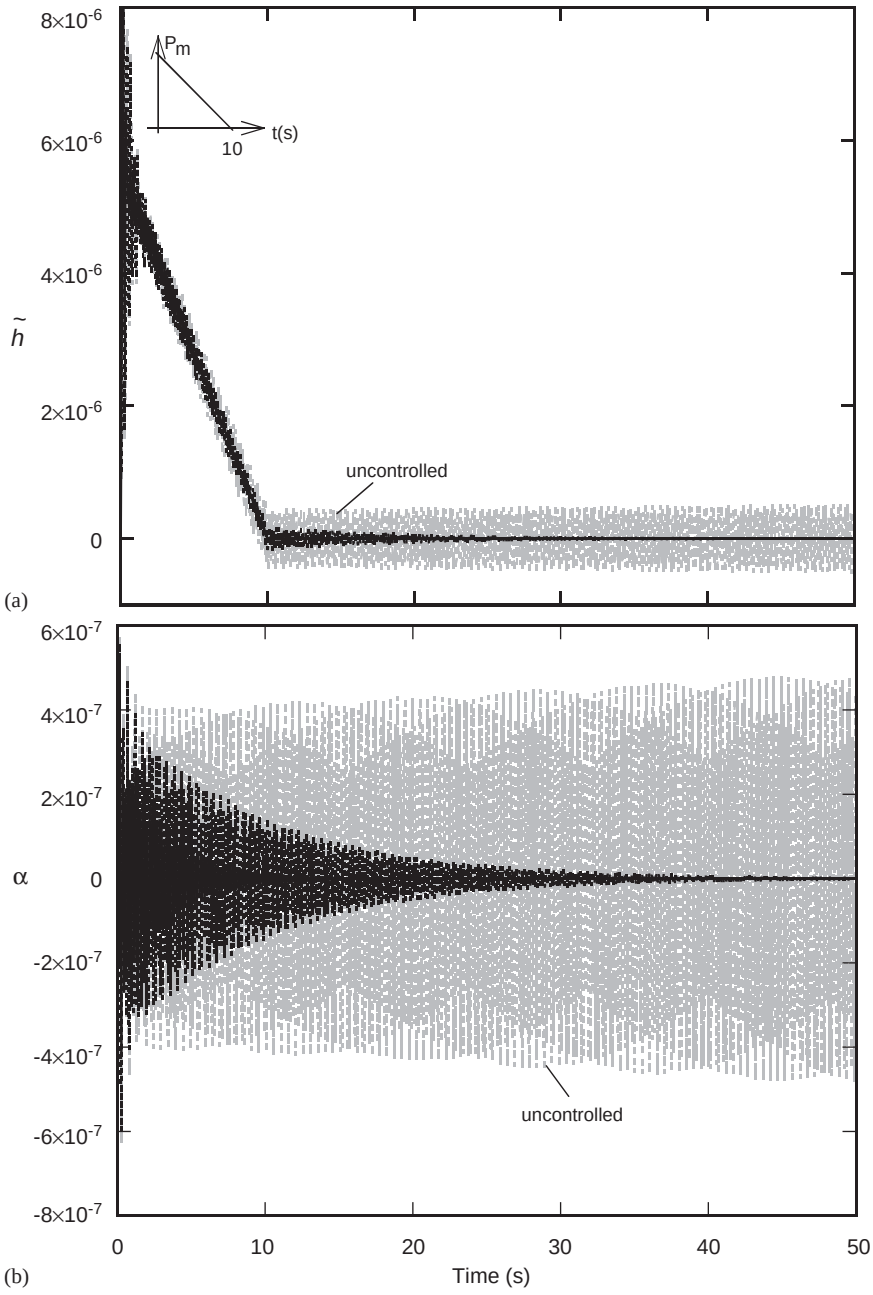

Fig. 2. (a) Open/closed-loop plunging time-history under an explosive blast ($t_p = 10$ s): ....., $g_{\dot{\alpha}} = 0.3$; ——-, $g_{\dot{\alpha}} = g_{\dot{h}} = 0.3$. Pitching and combined plunging/pitching velocity feedback control laws. (b) Pitching time-history counterpart.

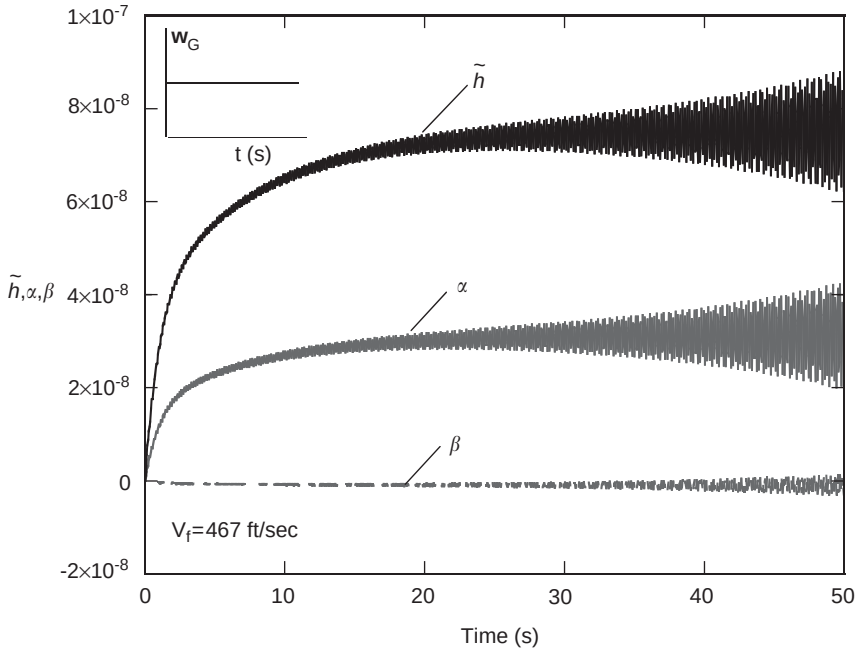

Fig. 3. Open-loop response of the aeroelastic system under a step pulse ($V_f = 467\,\mathrm{ft/s}$): h, plunging; α, pitching; β, flapping time-histories.

The results reveal that by increasing the feedback gains from $g_{\dot{h}} = g_{\dot{\alpha}} = 0.1$ to $g_{\dot{h}} = g_{\dot{\alpha}} = 0.2\,\mathrm{lb/(ft\ s)}$, the system is stabilized in a shorter time.

In Figs. 9 and 10 the influence on the dimensionless displacement time-histories in pitching and flapping to a graded gust load for control laws characterized by ($g_{\dot{h}} = 0.05$, $0.3\,\mathrm{lb/(ft\ s)}$) and ($g_{\dot{\alpha}} = 0.1$, $0.3\,\mathrm{lb/(ft\ s)}$) are presented. In both cases, for flight speeds larger than the flutter speed, the system remains unstable even in the presence of the control.

The optimal control methodology is likely to be more effective from the point of view of the performance of the control. Fig. 11 displays the open/closed-loop pitching aeroelastic time-histories of the airfoil impacted by a step pulse for selected values of the flight speed. From this plot the high efficiency of the application of the LQR toward stabilizing the airfoil operating at the flutter speed is appearing. Also this result has been validated; see Refs. [9,10]. On the same plot, also the uncontrolled response for $V_f = V_F$ is presented.

For the same type of external excitation, Fig. 12 shows that for the control input considered here, whereas FLC ($\mathrm{sc}_1 = 9 \times 10^7$; $\mathrm{sc}_2 = 1 \times 10^7$; $\mathrm{sc}_3 = 3 \times 10^{-7}$) is not able to stabilize the system, MBB ($u_{\max} = 3 \times 10^{-7}\,\mathrm{lb/ft}$) proves to be highly efficient towards its stabilization.

In Figs. 13(a) and (b) the performance of the application of the LQR and MBB to stabilize the pitching aeroelastic response of the airfoil exposed to a step pulse are presented. While in Fig. 13(a), $u_{\max} = 3 \times 10^{-7}\,\mathrm{lb/ft}$, in Fig. 13(b), $u_{\max} = 3 \times 10^{-8}\,\mathrm{lb/ft}$. Both control methodologies appear to be very successful. However, as it appears from Fig. 13(b) for which a lower control

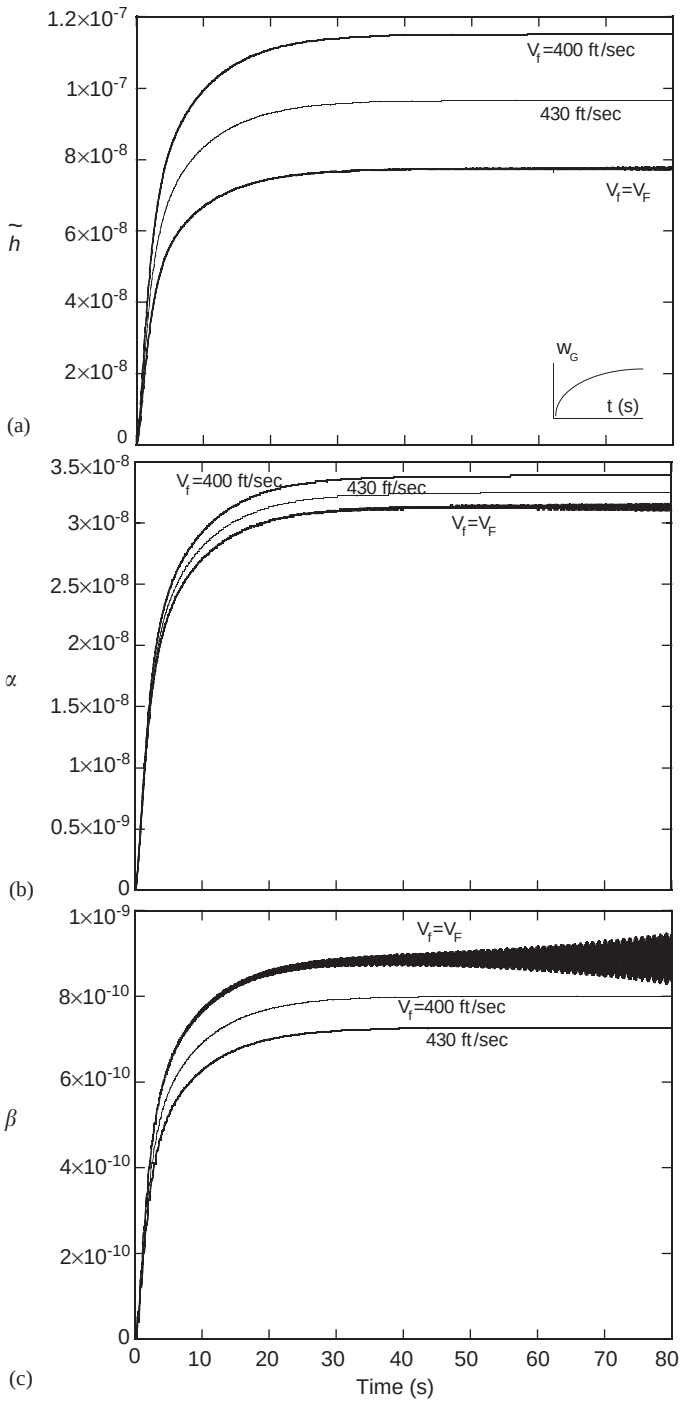

Fig. 4. (a) Open-loop plunging ($\tilde{h}$) aeroelastic response of the aeroelastic system under a graded gust for selected flight speeds. (b) The counterpart in pitching (α). (c) The counterpart in flapping (β).

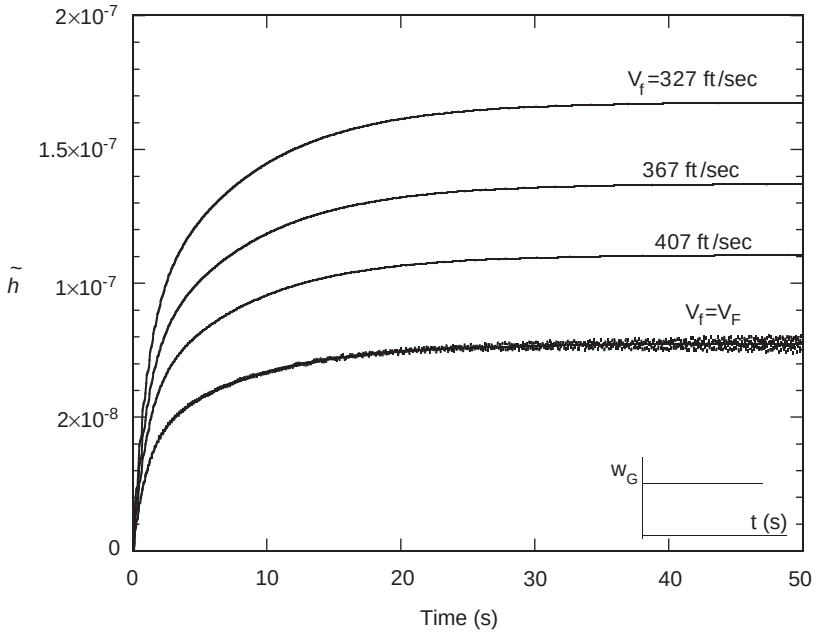

Fig. 5. Open/closed-loop plunging time-history of the aeroelastic system under a step pulse for selected flight speeds. Effect of the control. ....., uncontrolled; ——, controlled.

input was considered, the MBB control methodology appears more efficient than the LQR that is not able to stabilize the aeroelastic system.

It is worth remarking that the methodology presented here can be extended to the compressible flight speed regimes. In this sense, proper aerodynamic indicial functions for the compressible subsonic, supersonic and hypersonic flight speed regimes have to be applied; see Refs. [21–24]. However, the goal of this paper was restricted to the issue of the illustration of the methodology and to that of highlighting the importance of the implementation of the active control on the lifting surfaces equipped with a flap.

5. Conclusions

Results related to the aeroelastic response and control of 2-D wing-flap systems operating in an incompressible flight speed and exposed to blast/gust loads are presented. Plunging/pitching velocity feedback controls and combined controls, as well as optimal control methodologies such as LQR, MBB and FLC are considered, and their relative performances are highlighted. It clearly appears that, in addition to its inherent virtues of involving a constraint in the control input, MBB appears to be more efficient than LQR, FLC and the velocity feedback control methodologies. Dealing with the aeroelastic response, the necessity of addressing it in the time-domain becomes evident. As a result, the aerodynamics based on the concept of the aerodynamic indicial function

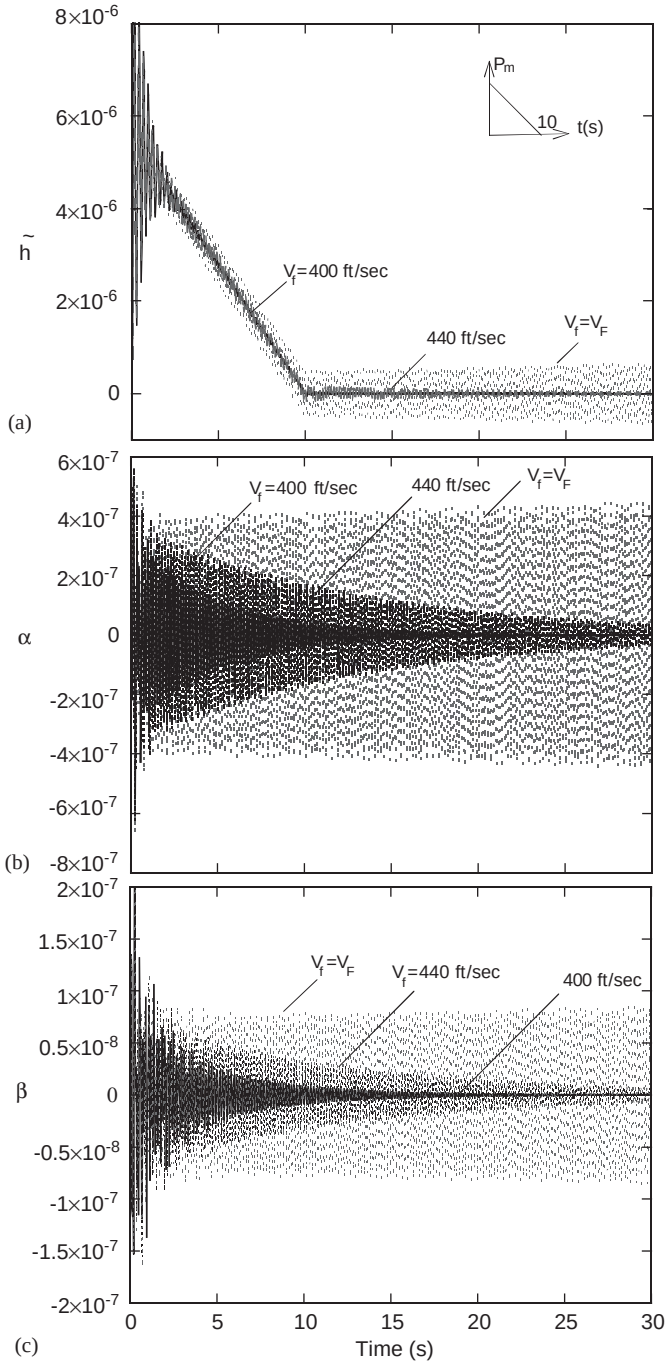

Fig. 6. (a) Open-loop response of the aeroelastic system under an explosive blast ($t_p = 10$ s), for selected flight speeds. Plunging ($\tilde{h}$) time-history. (b) Pitching (α) time-history counterpart. (c) Flapping (β) time-history counterpart.

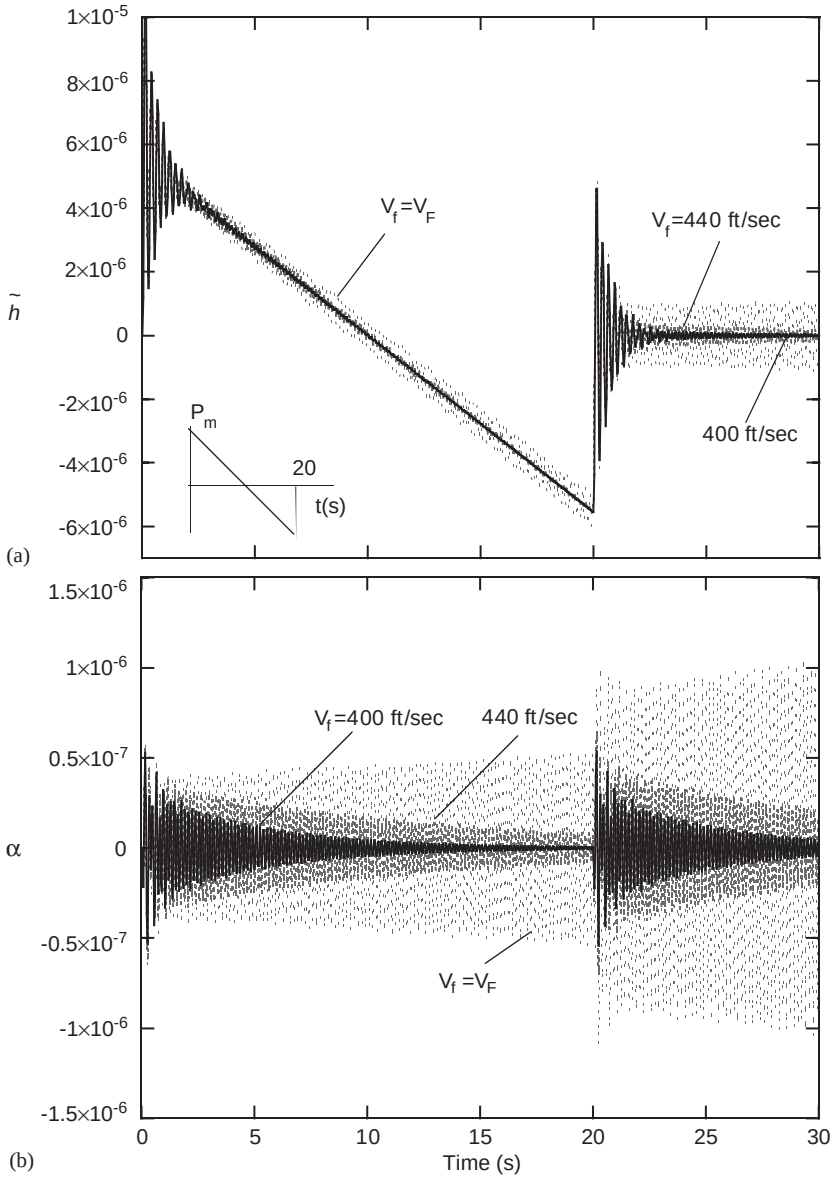

Fig. 7. (a) Open-loop plunging ($\tilde{h}$) time-history response of the aeroelastic system under a sonic-boom pulse for selected flight speeds ($t_p = 10\,\text{s}$, $r = 2$). (b) Pitching (α) time-history counterpart.

not only indicate that they are most appropriate for addressing this problem, but in addition, prove to be of great efficiency. Moreover, its use can be extended to various flight speed regimes, i.e. compressible subsonic, transonic and supersonic, and as a result, an unified approach

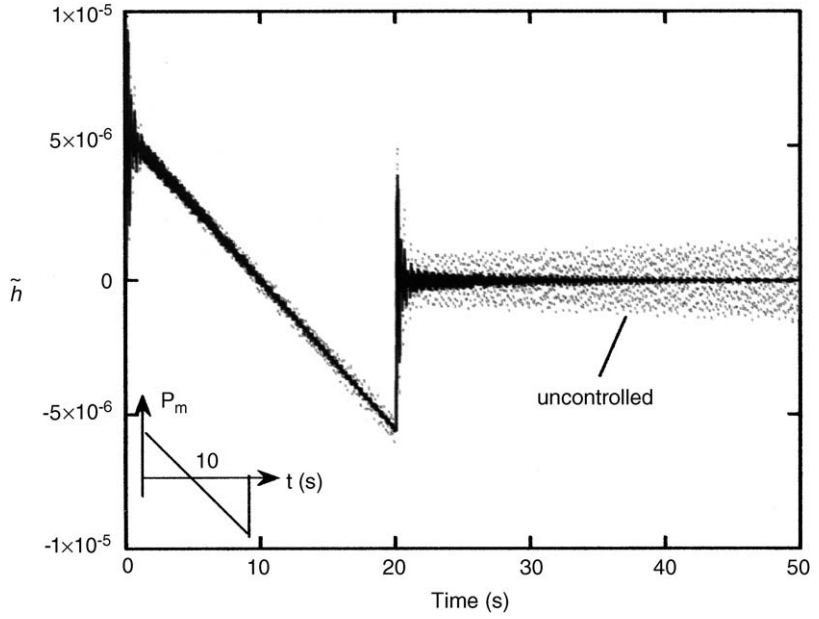

Fig. 8. Open/closed-loop plunging time-history of the aeroelastic system under a sonic-boom pulse ($t_p = 10\,\mathrm{s}$, $r = 2$). Plunging/pitching and combined velocity feedback control laws. ....., $g_{\dot{h}} = g_{\dot{\alpha}} = 0.1$; ——, $g_{\dot{h}} = g_{\dot{\alpha}} = 0.2$.

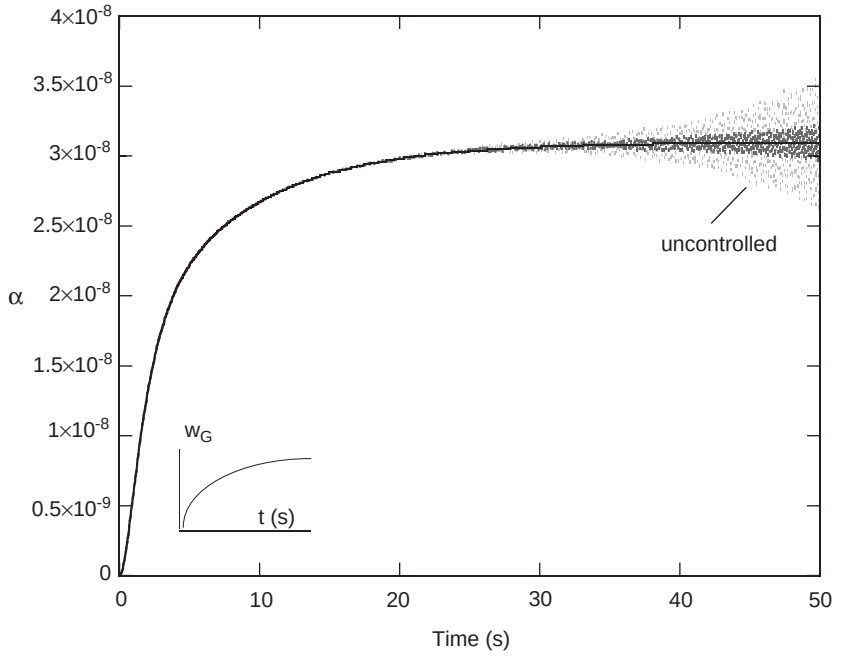

Fig. 9. Open/closed-loop pitching time-history of the aeroelastic system under a graded gust. Plunging velocity feedback control. ....., $g_{\dot{h}} = 0.05$; ——, $g_{\dot{h}} = 0.3$.

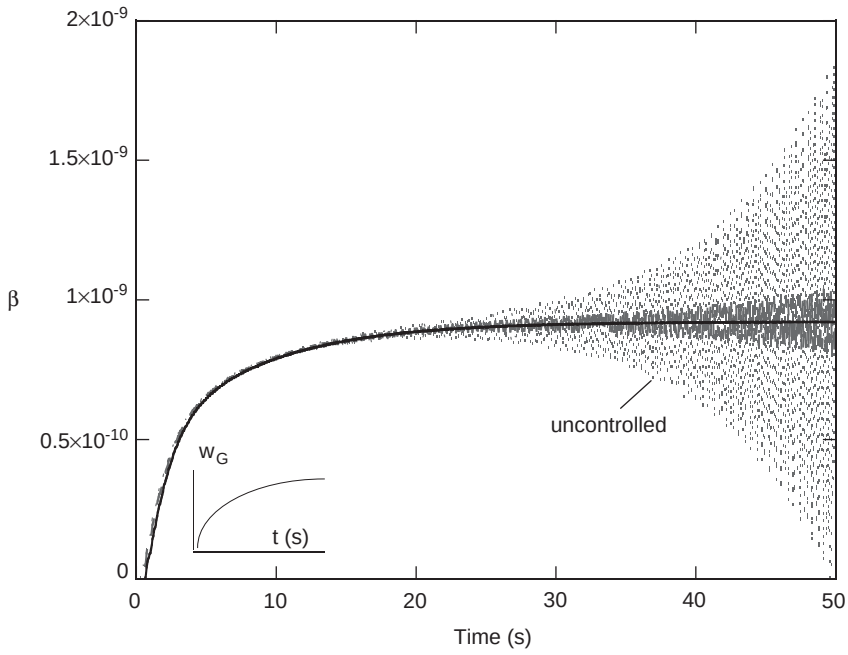

Fig. 10. Open/closed-loop flapping time-history of the aeroelastic system under a graded gust. Pitching velocity feedback control. ....., $g_{\dot{\alpha}} = 0.1$; ——, $g_{\dot{\alpha}} = 0.3$.

of this problem becomes feasible. Results addressing these additional issues will be presented elsewhere.

Acknowledgements

L. Librescu and P. Marzocca would like to acknowledge the partial support by the NASA Langley Research Center through Grant NAG-1-02-011. S.S. Na and M.K. Kwak also acknowledge the partial support by the Basic Research Program of the Korea Science and Engineering Foundation, Grant No. R01-2002-000-00129-0. The authors express their indebtedness to the anonymous reviewers for the constructive comments and suggestions that have contributed to the improvement of the paper.

Appendix A. Flutter and aeroelastic response

In order to be reasonably self-contained, a few steps enabling one to obtain the flutter and aeroelastic response are provided here. Detailed developments are supplied in Ref. [18,20,21].

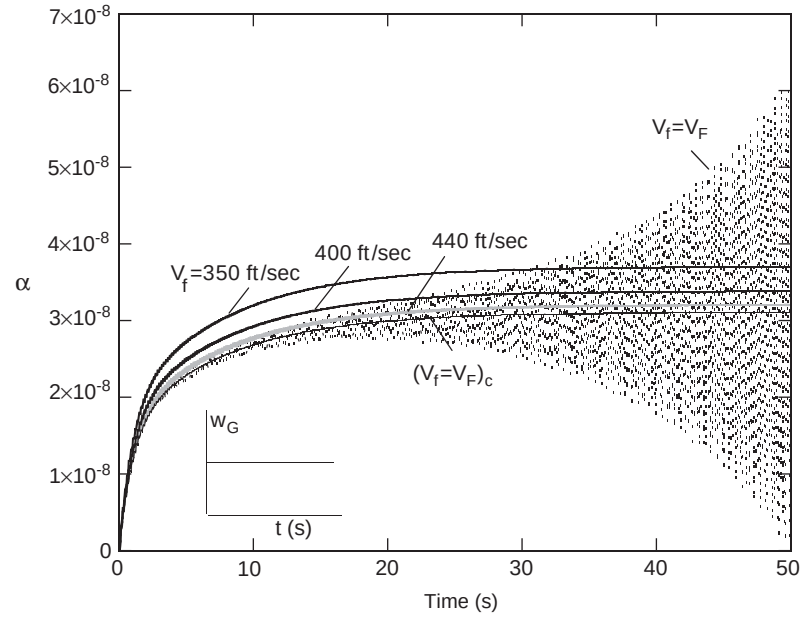

Fig. 11. Open/closed-loop (LQR) pitching time-history of the aeroelastic system under a step pulse for selected flight speeds. ....., uncontrolled; ——, controlled.

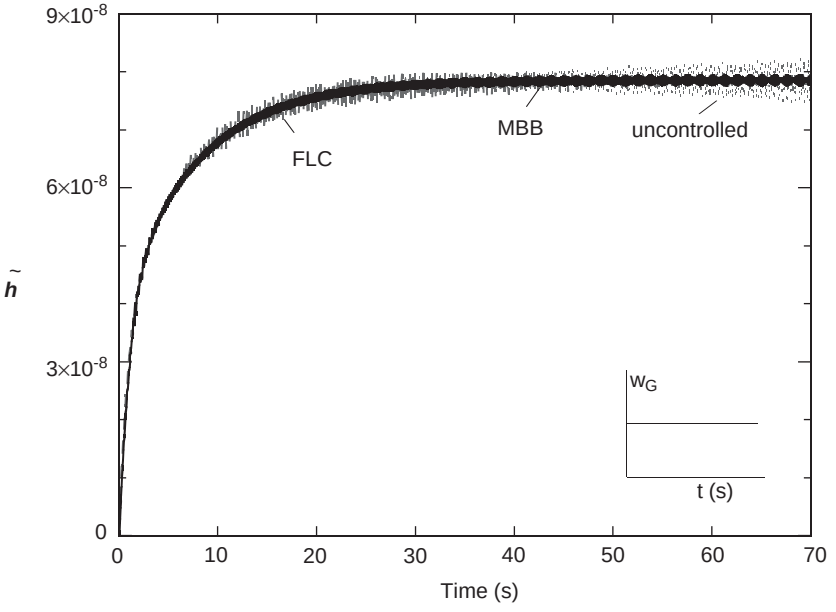

Fig. 12. Open/closed-loop (MBB and FLC) plunging time-history of the aeroelastic system under a step pulse: ....., FLC; ——, MBB.

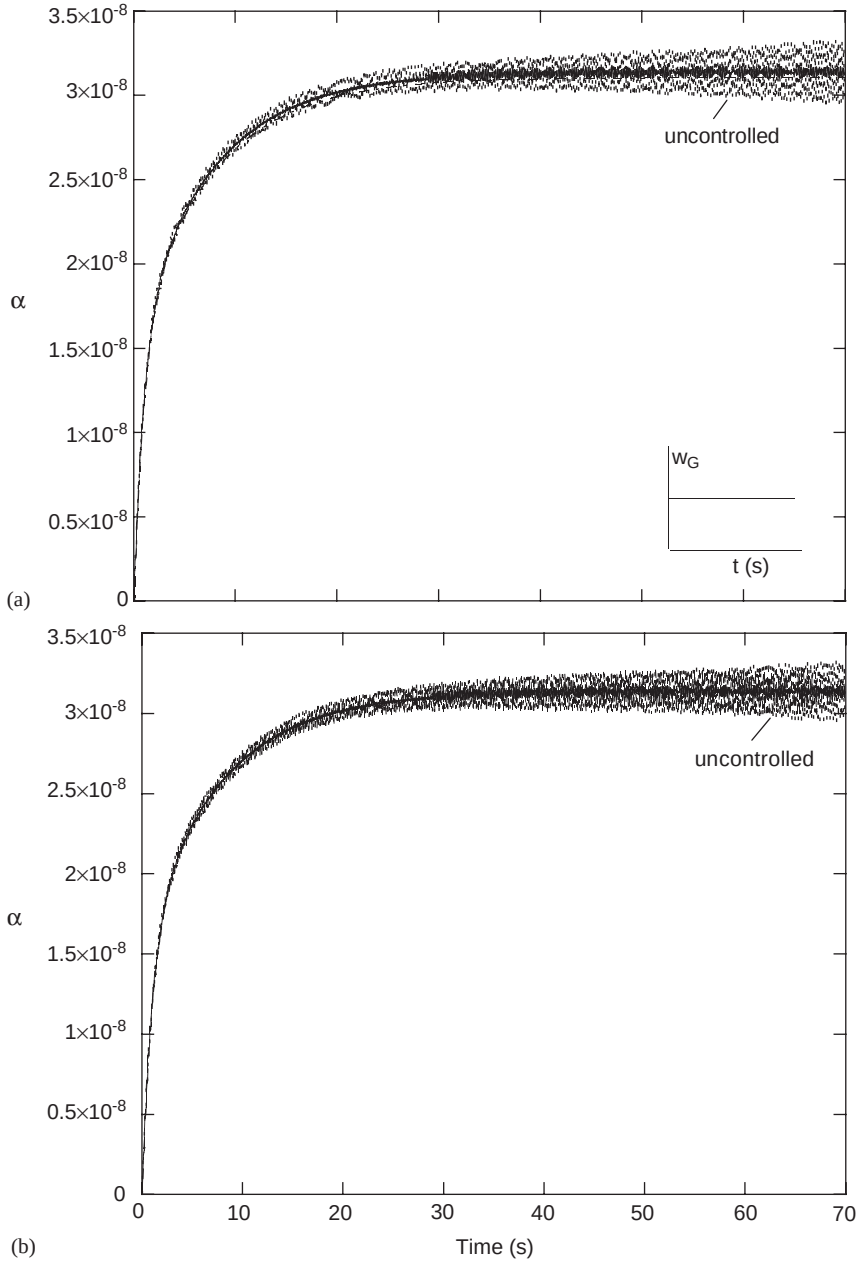

Fig. 13. Open/closed-loop (MBB and LQR) pitching time-history of the aeroelastic system under a step pulse: ....., LQR; ——, MBB. (a) $u_{\max} = 3 \times 10^{-7}$ lb/ft, (b) $u_{\max} = 3 \times 10^{-8}$ lb/ft.

The 10 first-order simultaneous differential equations of the aeroelastic airfoil-flap system can be represented in the form

$$\dot{\mathbf{X}}(t)=\frac{\mathrm{d}}{\mathrm{d}t}\begin{Bmatrix}\dot{\mathbf{Y}}(t)\\ \mathbf{Y}(t)\\ \mathbf{x_A}(t)\end{Bmatrix}=\begin{Bmatrix}\ddot{\mathbf{Y}}(t)\\ \dot{\mathbf{Y}}(t)\\ \dot{\mathbf{x}}_{\mathbf{A}}(t)\end{Bmatrix}=\mathbf{A}\begin{Bmatrix}\dot{\mathbf{Y}}(t)\\ \mathbf{Y}(t)\\ \mathbf{x_A}(t)\end{Bmatrix}+\mathbf{Bu}(t)+\mathbf{G}_g\mathbf{w}_g(t)+\mathbf{G}_b\mathbf{w}_b(t), \tag{A.1}$$

where $\mathbf{x_A}(t)$ contains the four aerodynamic state variables:

$$\mathbf{x_A}(t)=[B_1(t)\quad B_2(t)\quad A_1(t)\quad A_2(t)]^{\mathrm{T}}. \tag{A.2}$$

The aerodynamic matrix is given as

$$\overset{10\times10}{\mathbf{A}}=\begin{bmatrix}\mathbf{A_{11}} & \mathbf{A_{12}} & \mathbf{A_{13}}\\ \mathbf{A_{21}} & \mathbf{A_{22}} & \mathbf{A_{23}}\\ \mathbf{A_{31}} & \mathbf{A_{32}} & \mathbf{A_{33}}\end{bmatrix}. \tag{A.3}$$

Notice that $\mathbf{A}_{ij}$ is the submatrix of $\mathbf{A}$. Collecting the terms, the open-loop governing equation reduces to

$$\begin{aligned}[\mathbf{M}+\pi\rho b^2\mathbf{Z_1}]\ddot{\mathbf{Y}}(t)=&-\mathbf{KY}(t)-\pi\rho b^2\{\mathbf{Z_2}\dot{\mathbf{Y}}(t)+\mathbf{Z_3}\mathbf{Y}(t)+\mathbf{Z_4}\mathbf{x_A}(t)\}\\ &-\pi\rho b^3\begin{bmatrix}1&0&0\\0&1&0\\0&0&1\end{bmatrix}\begin{Bmatrix}w_L(t)+f(t)\\ w_M(t)\\ w_f(t)\end{Bmatrix}.\end{aligned} \tag{A.4}$$

This system of equations can be solved for $\ddot{\mathbf{Y}}(t)$:

$$\begin{aligned}\ddot{\mathbf{Y}}(t)=&-[\mathbf{M}+\pi\rho b^2\mathbf{Z_1}]^{-1}\{\pi\rho b^2\mathbf{Z_2}\dot{\mathbf{Y}}(t)+(\mathbf{K}+\pi\rho b^2\mathbf{Z_3})\mathbf{Y}(t)+\pi\rho b^2\mathbf{Z_4}\mathbf{x_A}(t)\}\\ &-\pi\rho b^3[\mathbf{M}+\pi\rho b^2\mathbf{Z_1}]^{-1}\begin{bmatrix}1&0&0\\0&1&0\\0&0&1\end{bmatrix}\begin{Bmatrix}w_L(t)+f(t)\\ w_M(t)\\ w_f(t)\end{Bmatrix}.\end{aligned} \tag{A.5}$$

The model of the controlled lifting surface with flap under gust loads is given by

$$\begin{Bmatrix}\ddot{\mathbf{Y}}(t)\\ \dot{\mathbf{Y}}(t)\\ \dot{\mathbf{x}}_{\mathbf{A}}(t)\end{Bmatrix}=\mathbf{A}\begin{Bmatrix}\dot{\mathbf{Y}}(t)\\ \mathbf{Y}(t)\\ \mathbf{x_A}(t)\end{Bmatrix}-\mathbf{G}\begin{Bmatrix}w_L(t)+f(t)\\ w_M(t)\\ w_f(t)\end{Bmatrix}+\mathbf{Bu}(t), \tag{A.6}$$

where the disturbance-input matrix, $\mathbf{G}$, and the external disturbance vector, $\mathbf{w}(t)$, are defined as

$$\mathbf{G}=-\pi\rho b^3[\mathbf{M}+\pi\rho b^2\mathbf{Z_1}]^{-1}\begin{bmatrix}1&0&0\\0&1&0\\0&0&1\\ \multicolumn{3}{c}{\mathbf{0}_{7\times3}}\end{bmatrix}, \tag{A.7}$$

$$\mathbf{w}(t)=\{w_L(t)+f(t)\quad w_M(t)\quad w_f(t)\}^{\mathrm{T}}. \tag{A.8}$$

In addition, the following matrices are needed:

$$\mathbf{r_1} = [R_1 \quad R_2 \quad R_3], \quad \mathbf{r_2} = [0 \quad R_4 \quad R_5], \quad \mathbf{r_3} = [R_6 \quad R_7 \quad R_8], \quad \mathbf{r_4} = [0 \quad R_9 \quad R_{10}], \tag{A.9}$$

$$\overset{3\times3}{\mathbf{A_{11}}} = -[\mathbf{M} + \pi\rho b^2\mathbf{Z_1}]^{-1}\pi\rho b^2\mathbf{Z_2}, \quad \overset{3\times3}{\mathbf{A_{12}}} = -[\mathbf{M} + \pi\rho b^2\mathbf{Z_1}]^{-1}[\mathbf{K} + \pi\rho b^2\mathbf{Z_3}], \tag{A.10}$$

$$\overset{3\times4}{\mathbf{A_{13}}} = -[\mathbf{M} + \pi\rho b^2\mathbf{Z_1}]^{-1}\pi\rho b^2\mathbf{Z_4}, \quad \mathbf{A_{21}} = \mathbf{I}_{3\times3}, \quad \mathbf{A_{22}} = \mathbf{0}_{3\times3}, \quad \mathbf{A_{23}} = \mathbf{0}_{3\times4}, \tag{A.11}$$

$$\overset{4\times3}{\mathbf{A_{31}}} = \begin{bmatrix} \mathbf{r_1A_{11}} + \mathbf{r_2} \\ \mathbf{r_1A_{11}} + \mathbf{r_2} \\ \mathbf{r_3A_{11}} + \mathbf{r_4} \\ \mathbf{r_3A_{11}} + \mathbf{r_4} \end{bmatrix}, \quad \overset{4\times3}{\mathbf{A_{32}}} = \begin{bmatrix} \mathbf{r_1A_{12}} \\ \mathbf{r_1A_{12}} \\ \mathbf{r_3A_{12}} \\ \mathbf{r_3A_{12}} \end{bmatrix}, \tag{A.12}$$

$$\overset{4\times4}{\mathbf{A_{33}}} = \begin{bmatrix} \frac{-\beta_1 V_f}{b} & 0 & 0 & 0 \\ 0 & \frac{-\beta_2 V_f}{b} & 0 & 0 \\ 0 & 0 & \frac{-\beta_1 V_f}{b} & 0 \\ 0 & 0 & 0 & \frac{-\beta_2 V_f}{b} \end{bmatrix} + \begin{bmatrix} \mathbf{r_1A_{13}} \\ \mathbf{r_1A_{13}} \\ \mathbf{r_3A_{13}} \\ \mathbf{r_3A_{13}} \end{bmatrix}. \tag{A.13}$$

In Eqs. (A.10) and (A.11),

$$\mathbf{Z_1} = \begin{bmatrix} L_{\ddot{h}} & L_{\ddot{\alpha}} & L_{\ddot{\beta}} \\ M_{\ddot{h}} & M_{\ddot{\alpha}} & M_{\ddot{\beta}} \\ T_{\ddot{h}} & T_{\ddot{\alpha}} & T_{\ddot{\beta}} \end{bmatrix}, \quad \mathbf{Z_2} = \begin{bmatrix} L_{\dot{h}} & L_{\dot{\alpha}} & L_{\dot{\beta}} \\ 0 & M_{\dot{\alpha}} & M_{\dot{\beta}} \\ T_{\dot{h}} & T_{\dot{\alpha}} & T_{\dot{\beta}} \end{bmatrix}, \tag{A.14}$$

$$\mathbf{Z_3} = \begin{bmatrix} 0 & L_\alpha & L_\beta \\ 0 & 0 & M_\beta \\ 0 & T_\alpha & T_\beta \end{bmatrix}, \quad \mathbf{Z_4} = \begin{bmatrix} L_{B_1} & L_{B_2} & 0 & 0 \\ 0 & 0 & 0 & 0 \\ 0 & 0 & T_{A_1} & T_{A_2} \end{bmatrix}, \tag{A.15}$$

$$\{-L(t) \quad -M(t) \quad -T(t)\}^{\mathrm{T}} = -\pi\rho b^2\{\mathbf{Z_1}\ddot{\mathbf{Y}}(t) + \mathbf{Z_2}\dot{\mathbf{Y}}(t) + \mathbf{Z_3}\mathbf{Y}(t) + \mathbf{Z_4}\mathbf{x_A}(t)\}. \tag{A.16}$$

Concerning the coefficients R_i appearing in Eqs. (A.9), these are defined in terms of the Φ_i coefficients derived in Ref. [16], and on the flight and geometrical parameters

$$\begin{aligned} &R_1 = \frac{b^2}{V_f}, \quad R_2 = \frac{b^2}{V_f}\left(\tfrac{1}{2} - x_{\mathrm{EA}}\right), \quad R_3 = \frac{\Phi_2 b^2}{2\pi V_f}, \quad R_4 = V_f, \\ &R_5 = \frac{\Phi_1 V_f}{\pi}, \quad R_6 = \frac{\Phi_8 b^3}{\pi V_f}, \quad R_7 = \frac{\Phi_8 b^3}{\pi V_f}\left(\frac{1}{2} - x_{\mathrm{EA}}\right), \\ &R_8 = \frac{\Phi_2\Phi_8 b^3}{2V_f\pi^2}, \quad R_9 = \frac{\Phi_8 V_f b}{\pi}, \quad R_{10} = \frac{\Phi_1\Phi_8 V_f b}{\pi^2}. \end{aligned} \tag{A.17}$$

The first-order differential equation for the aerodynamic lag states is written as [19,20]

$$\dot{\mathbf{x}}_\mathbf{A}(t) = \mathbf{P}\mathbf{x}_\mathbf{A}(t) + \dot{\mathbf{Q}}, \tag{A.18}$$

or in a detailed form:

$$\dot{\mathbf{x}}_{\mathbf{A}}(t) = \left\{ \dot{B}_1(t) \quad \dot{B}_2(t) \quad \dot{A}_1(t) \quad \dot{A}_2(t) \right\}^{\mathrm{T}} = \begin{bmatrix} \frac{-\beta_1 V_f}{b} & 0 & 0 & 0 \\ 0 & \frac{-\beta_2 V_f}{b} & 0 & 0 \\ 0 & 0 & \frac{-\beta_1 V_f}{b} & 0 \\ 0 & 0 & 0 & \frac{-\beta_2 V_f}{b} \end{bmatrix} \begin{Bmatrix} B_1(t) \\ B_2(t) \\ A_1(t) \\ A_2(t) \end{Bmatrix} + \begin{Bmatrix} \dot{Q}_1(t) \\ \dot{Q}_1(t) \\ \dot{Q}_2(t) \\ \dot{Q}_2(t) \end{Bmatrix}, \tag{A.19}$$

$$\dot{Q}_1(t) = \{R_1 \quad R_2 \quad R_3\}\ddot{\mathbf{Y}}(t) + \{0 \quad R_4 \quad R_5\}\dot{\mathbf{Y}}(t) = \mathbf{r_1}\ddot{\mathbf{Y}}(t) + \mathbf{r_2}\dot{\mathbf{Y}}(t), \tag{A.20}$$

$$\dot{Q}_2(t) = \{R_6 \quad R_7 \quad R_8\}\ddot{\mathbf{Y}}(t) + \{0 \quad R_9 \quad R_{10}\}\dot{\mathbf{Y}}(t) = \mathbf{r_3}\ddot{\mathbf{Y}}(t) + \mathbf{r_4}\dot{\mathbf{Y}}(t). \tag{A.21}$$

In the time domain the aerodynamic loads have the form presented in Eqs. (12)–(14). As stated in Refs. [19,20], the formulation presented here eliminates the need of evaluating the Duhamel integrals. In this sense, the aerodynamic governing equations reduces to a system of first-order differential equation.

References

[1] P. Marzocca, L. Librescu, G. Chiocchia, Aeroelastic response of a 2-D lifting surfaces to gust and arbitrary explosive loading signatures, *International Journal of Impact Engineering* 25 (2001) 41–65.

[2] P. Marzocca, L. Librescu, G. Chiocchia, Aeroelasticity of two-dimensional lifting surfaces via indicial function approach, *The Aeronautical Journal* 106 (2002) 147–153.

[3] H. Horikawa, E.H. Dowell, An elementary explanation of the flutter mechanism with active feedback controls, *Journal of Aircraft* 16 (1979) 225–232.

[4] J.S. Vipperman, R.L. Clark, M.D. Conner, E.H. Dowell, Investigation of the experimental active control of a typical section airfoil using a trailing edge flap, *Journal of Aircraft* 35 (1998) 224–229.

[5] K. Lazaraus, E. Crawley, C. Lin, Fundamental mechanisms of aeroelastic control with control surface and strain actuation, *Journal of Guidance, Control, and Dynamics* 18 (1995) 10–17.

[6] V. Mukhopadhyay, Historical perspective on analysis and control of aeroelastic responses, *Journal of Guidance, Control, and Dynamics* 26 (2003) 673–684.

[7] V. Mukhopadhyay, Flutter suppression control law design and testing for the active flexible wing, *Journal of Aircraft* 32 (1995) 45–51.

[8] V. Mukhopadhyay (Ed.), Benchmark active control technology, *Journal of Guidance, Control, and Dynamics*, Part I 23 (2000) 913–960; Part II 23 (2000) 1093–1139; Part III 24 (2001) 146–192.

[9] S.S. Na, L. Librescu, Optimal vibration control of a thin-walled anisotropic cantilevers exposed to blast loading, *Journal of Guidance, Control, and Dynamics* 23 (2000) 491–500.

[10] S.S. Na, L. Librescu, Oscillation control of cantilevers via smart materials technology and optimal feedback control: actuator location and power consumption issues, *Smart Materials and Structures* 7 (1998) 833–842.

[11] L. Librescu, S.S. Na, Bending vibration control of cantilevers via boundary moment and combined feedback control laws, *Vibration and Controls* 4 (1998) 733–746.

[12] J.C. Bruch Jr., J.M. Sloss, S. Adali, I.S. Sadek, Modified bang-bang piezoelectric control of vibrating beams, *Smart Materials and Structures* 8 (1999) 647–653.

[13] L. Librescu, S.S. Na, S. Kim, Comparative study on vibration control methodologies applied to adaptive anisotropic cantilevers, *Proceedings of the 43nd AIAA/ASME/ASCE/ASC Structures, Structural Dynamics, and Materials Conference*, AIAA-2002-1539, Denver, 2002.
[14] R.H. Scanlan, R. Rosenbaum, *Introduction to the Study of Aircraft Vibration and Flutter*, Macmillian, New York, 1951.
[15] J.W. Edwards, Unsteady aerodynamic modeling and active aeroelastic control, SUDARR 504 (NASA Grant ngl-05-020-007), Stanford University, February 1977. Also available as NASA CR-148019.
[16] H.G. Kussner, I. Schwarz, The oscillating wing with aerodynamically balanced elevator, NACA-TM991, October 1941.
[17] S.D. Olds, Modeling and LQR Control of a Two-Dimensional Airfoil, MS Thesis, Department of Mathematics, Virginia Polytechnic Institute and State University, Blacksburg, VA, April 1997.
[18] E.H. Dowell, *A Modern Course in Aeroelasticity*, Sijthoff and Noordhoff, Alphen a/d Rejn Rejn, 1978.
[19] W.P. Rodden, B. Stahl, A strip method for prediction of damping in subsonic wind tunnel and flight flutter tests, *Journal of Aircraft* 6 (1969) 9–17.
[20] D.L. York, Analysis of Flutter and Flutter Suppression via an Energy Method, MS Thesis, Department of Aerospace and Ocean Engineering, Virginia Polytechnic Institute and State University, Blacksburg, VA, May 1980.
[21] J.G. Leishman, Unsteady lift of an airfoil with a trailing-edge flap based on indicial concepts, *Journal of Aircraft* 31 (1994) 288–297.
[22] P. Marzocca, L. Librescu, G. Chiocchia, Aeroelastic response of a 2-D airfoil in compressible flight speed regimes exposed to blast loadings, *Aerospace Science and Technology* 6 (2002) 259–272.
[23] Z. Qin, P. Marzocca, L. Librescu, Aeroelastic instability and response of advanced aircraft wings at subsonic flight speeds, *Aerospace Science and Technology* 6 (2002) 195–208.
[24] P. Marzocca, L. Librescu, W.A. Silva, Flutter, post-flutter and control of a supersonic 2-D lifting surface, *Journal of Guidance, Control, and Dynamics* 25 (2002) 962–970.
[25] J.A. Drischler, F.W. Diederich, Lift and moment responses to penetration of sharp-edged traveling gusts, with application to penetration of weak blast waves, NACA Technical Note 3956, 1957.
[26] R. Lomax, Lift developed on unrestrained rectangular wings entering gusts at subsonic and supersonic speeds, NACA Technical Note 2925, 1953.
[27] R. Lomax, M.A. Reaslet, F.B. Fuller, L. Sluder, Two and three dimensional unsteady lift problems in high speed flight, NACA Report 1077, 1952.
[28] J.G. Leishman, Unsteady aerodynamics of airfoils encountering traveling gusts and vortices, *Journal of Aircraft* 34 (1997) 719–729.
[29] L. Djayapertapa, C.B. Allen, Numerical simulation of active control of transonic flutter, *Proceedings of the 23rd ICAS Congress*, Toronto, 2002, pp. 411.1–411.10.